Keyhole limpet hemocyanin: Structural and functional characterization of two different subunits and multimers

ARTICLE *in* COMPARATIVE BIOCHEMISTRY AND PHYSIOLOGY PART B BIOCHEMISTRY AND MOLECULAR BIOLOGY · APRIL 1996

Impact Factor: 1.55 · DOI: 10.1016/0305-0491(95)02091-8 · Source: PubMed

Comp. Biochem. Physiol. Vol. 113B, No. 3, pp. 537–548, 1996

ISSN 0305-0491/96/$15.00
SSDI 0305-0491(95)02091-8

Keyhole Limpet Hemocyanin: Structural and Functional Characterization of Two Different Subunits and Multimers

Richard D. Swerdlow,[1] Ray F. Ebert,[2] Psyche Lee,[3] Celia Bonaventura[4] and Karen I. Miller[5]

[1]PERIMMUNE, INC., ROCKVILLE, MD, [2]AMERICAN RED CROSS, ROCKVILLE, MD, [3]DUKE UNIVERSITY MEDICAL CENTER, DURHAM, NC, [4]DUKE UNIVERSITY MARINE BIOMEDICAL CENTER, BEAUFORT, NC AND [5]OREGON STATE UNIVERSITY, CORVALLIS, OR, USA

ABSTRACT. Keyhole limpet hemocyanin (KLH), the large respiratory glycoprotein from the primitive gastropod mollusc, *Megathura crenulata*, is a potent immunogen used classically as a carrier protein for haptens and more recently in human vaccines and for immunotherapy of bladder cancer. Two KLH isoforms were identified and isolated by high-performance anion exchange chromatography. Subsequent analyses disclosed that these isoforms—designated KLH-A and KLH-B—were composed of distinct subunits that differed in primary structure, molecular weight (KLH-A was 449,000 and KLH-B was 392,000), polymerization/reassociation characteristics, and O_2-binding constants (KLH-A had a P_{50} of 7.32 and KLH-B had a P_{50} of 2.46). Both subunits appear to be composed of eight oxygen binding domains, and reassociate in solution only with like subunits. These results support the concept that structural and functional heterogeneity is a common feature of molluscan hemocyanins, and provide a rational basis for studying and optimizing the immunostimulatory properties of KLH. COMP BIOCHEM PHYSIOL 113B, 537–548, 1996.

KEY WORDS. Hemocyanin, mollusc, subunit heterogeneity, purification, molecular weight, amino acid composition, N-terminal sequence, oxygen binding, reassociation

INTRODUCTION

First described in 1878 by French naturalist Leon Frederiq (15), hemocyanins (from the Greek *haima* blood, and *kyanos* blue pigment) are blue colored glycoproteins present in two invertebrate phyla, Arthropoda and Mollusca. They function as respiratory proteins by virtue of their ability to bind oxygen in unique active sites that each contain two copper atoms (12,17,44,45).

Although they share the same name and function, arthropod and molluscan hemocyanins have evolved independently, as evidenced by major differences in size and composition of their subunits (21,44,45,46). Arthropod hemocyanins have ~75 kDa subunits with one O_2 binding site that assemble to form hexameric and multi-hexameric structures with molecular weights ranging from ~450 kDa to as high as ~4×10^6 Da. Molluscan hemocyanins have ~350–500 kDa subunits with 7 or 8 O_2 binding sites that assemble to decameric and multi-decameric structures of truly enormous size. Decamers of 3.5 to 5×10^6 Da; multidecamers can be two to several times that large. Conditions that are known to influence hemocyanin size distribution include ionic strength, pH, temperature, pO_2, and the availability of certain divalent cations, notably calcium and magnesium. It has been suggested that this property of self association provides a means by which extremely high respiratory protein concentrations can be achieved without a correspondingly adverse effect on hemolymph osmolarity.

Hemocyanin from *Megathura crenulata* is commonly referred to as keyhole limpet hemocyanin (KLH), even though M. *crenulata* is only one of many genera of the primitive gastropod family known as the Fissurellidae or keyhole limpets. KLH has been widely used in immunobiology, in large part because it is an extremely potent antigen. A single intracutaneous injection of KLH elicits a strong antibody response in virtually 100% of vertebrate animals, including humans (7,10,35,39). Conjugation of nonimmunogenic peptides or other haptens to KLH produces a preparation that rarely fails to stimulate antibody production against the target molecule. KLH also has been applied to the study of humoral and cellular immune responses in humans (4,7,8), and currently is under investigation as a carrier for an AIDS vaccine (25) and for a prophylactic vaccine to prevent cocaine abuse (2). In addition, recent results from human clinical trials have suggested that KLH

Address reprint requests to: Karen I. Miller, Department of Biochemistry and Biophysics, Oregon State University, Corvallis, OR 97331.

Received 21 March 1995; revised 22 August 1995; accepted 31 August 1995.

may be an effective immunotherapeutic agent against bladder cancer recurrences (14,24,26).

Despite its obvious potential for health-related applications and evidence that different forms of KLH may have different effects on the immune system (1,3,19,22,48), little is known regarding the primary structure and functional characteristics of this protein. Early work showed it to contain two different subunits (41). More recent studies (34,40) confirmed this observation but proposed a model for assembly into multimers which was incompatible with our preliminary observations. Furthermore none of these early studies compared the unique structural and functional properties of the two forms. This, plus our own interest in immunotherapy with KLH (28,42), prompted the present investigation in which we present evidence that the two KLH subunits, found in the blood as two distinct multimeric isoforms, have markedly different structural and functional properties.

MATERIAL AND METHODS

Materials

KLH was obtained from Pacific Biomarine Laboratories, Venice CA as freshly collected hemolymph, shipped as a saturated $(NH_4)_2SO_4$ solution containing suspended KLH particles. All other reagents were of analytical grade or better.

Purification of KLH

The $(NH_4)_2SO_4$ slurry containing KLH (~30 mg/mL) was dissolved in Dulbecco's phosphate-buffered saline solution (PBS, Gibco, Grand Island, NY) to a concentration of 5–10 mg/ml. After centrifugation at 1200 × **g** for 20 min to remove undissolved material, the supernatant fraction was centrifuged at 43,000 × **g** for 12–18 h, and the pellet containing concentrated KLH was redissolved as above in PBS, and recentrifuged at 43,000 × **g**. The final pellet was redissolved in PBS and stored at 4°C at a concentration of 5–10 mg/ml. This fraction of hemocyanin, which was >95% pure by SDS-PAGE, will be referred to as purified KLH.

HP-IEC Isolation of KLH Isoforms

Purified KLH was applied to a Protein-Pak DEAE 5PW column (7.5 × 75 mm, Waters-Millipore; Milford, MA) at a flow rate of 1.0 ml/min. A 20 mM Imidazole-HCl buffer (pH 6.5) containing 1 mM $CaCl_2$ and 0.5 mM $MgCl_2$ (solvent A) and solvent A plus 0.5 M NaCl (solvent B) elution system was used as follows: Linear gradient from 0 to 30% solvent B (2 min); wash with 30% B (6 min); linear gradient from 30–60% B (10 min); wash with 60% B (10 min).

Dissociation-Reassociation of KLH

KLH was dissociated to its monomeric form by dialysis against EDTA containing buffers as described previously (29,41). All Tris and bicarbonate buffers were produced at the indicated tonic strengths (I) according to Long (32). Reassociation studies (Fig. 9) used 50 mM Glycine pH 9.6 with 10 mM EDTA (Gly/EDTA buffer) to dissociate, followed by 0.1 I Tris pH 7.6 with 50 mM $MgCl_2$ and 10 mM $CaCl_2$ to reassociate. Sedimentation equilibrium studies were conducted with KLH-A and -B by first dialyzing against 0.1 I Tris pH 8 and 10 mM EDTA, then against 0.1 I Bicarbonate pH 10.0 for KLH-B and pH 10.7 for KLH-A. These samples were checked for complete dissociation to subunits by sedimentation velocity before equilibrium runs were started.

Electrophoresis

SDS-polyacrylamide gel electrophoresis (SDS-PAGE; 27) was performed under reducing conditions on a 5–15% polyacrylamide gradient. Nondenaturing gel electrophoresis (6) was performed under dissociating conditions on a 4–20% polyacrylamide gradient, using a buffer containing 140 mM Tris, 90 mM Boric acid and 2.5 mM EDTA at pH 8.6. Prior to electrophoresis, samples were dissociated by incubation for 30 min in this same buffer. In this method, proteins migrate through a steep polyacrylamide gradient for a sufficiently long time that their rates of migration approach zero. This minimizes the effect of differing net charges of proteins, leaving migration essentially a function of size and shape. A plot of migration versus log molecular weight of the protein standards was linear (not shown). Preliminary experiments were performed to establish the conditions (33 h at 150 V) needed for the migration of KLH-A and -B to approach zero. Following electrophoresis, all gels were stained by Coomassie Blue R-250.

Analytical Ultracentrifugation

A Beckman Model XL-A analytical ultracentrifuge equipped with scanner optics was used to determine sedimentation coefficients and molecular weights. For sedimentation velocity typical run conditions were 16,000 RPM at 21°C, at a protein concentration of ~1.0 mg/ml. Data were analyzed using XL-A Ultrascan 2.34, software developed by Dr. Borries Demeler specifically for the new XL-A. In this program velocity data were analyzed using the method of van Holde and Weischet (47). Sedimentation equilibrium run conditions were 6,500 RPM at 21°C. Equilibrium data were fitted by a nonlinear least squares method included in the above software, using models for single or double component systems. Partial specific volumes for KLH-A and -B were assumed to be 0.728.

Peptide Mapping

Proteins were digested with endoproteinase Lys-C (Boehringer Mannheim) at an enzyme/substrate ratio of 1:100 (w/w) for 18 h at 37°C in 25 mM Tris-HCl buffer (pH 8.9) plus 5 mM EDTA and 5% (v/v) acetonitrile. The digests were analyzed on a Vydac C4 column (9.4 × 250 mm). A 0.1% trifluoro-

acetic acid/water (solvent A) and 0.1% trifluoroacetic acid/acetonitrile (solvent B) elution system was used with a linear gradient from 5–70% solvent B (65 min) at a flow rate of 2.0 ml/min. The column effluent was monitored at 214 nm.

Electron Microscopy

KLH samples (0.5 mg/ml) were applied to carbon-coated grids, stained with 2% uranyl acetate, and examined in a Phillips 420 electron microscope.

Oxygen Binding

Oxygen binding behavior was analyzed by tonometric methods (38) using the absorbance at 345 nm as a measure of oxygen saturation.

Other Methods

Protein concentrations were determined by the method of Lowry *et al.* (33) using bovine serum albumin as a standard. Protein sequencing and amino acid analyses were performed as described previously (29). Copper content was determined by inductively coupled plasma emission spectroscopy (Analytical Chemical Services of Columbia, Inc).

RESULTS

Purification of KLH Isoforms

There are a variety of well established procedures for isolating KLH decamers and multidecamers (5,22,41,48). The differential centrifugation method chosen for this study (22) yielded a pellet containing decamers and multidecamers, as shown by sedimentation analysis and electron microscopy. A single major protein band was observed on SDS-PAGE (Fig. 1A, lane 1). This protein band was identified as KLH by Western blot analysis using an anti-KLH rabbit serum (not shown). We and others have observed that KLH subunits exhibit anomalously rapid mobility in SDS-PAGE, which results in a considerable underestimate of the actual molecular weight. In this case, based on its relative mobility, the molecular weight was only 280,000, much less than is seen by other methods. Thus, other techniques were used to establish molecular weight. Minor protein bands with faster mobility were also observed, typically representing <2% of the total protein. They were identified as KLH related by their reaction with anti-KLH by Western blot analysis. The proportion of these minor bands increases upon storage of KLH at ambient or elevated temperatures, and their appearance at discrete, nonrandom intervals may reflect the presence of labile peptide bonds in extended linker regions connecting the more globular O_2 binding domains.

Purified KLH was also analyzed by non-denaturing gel electrophoresis under dissociating conditions. Although SDS gels showed only one band, nondenaturing gels disclosed two major protein bands with apparent molecular masses of approximately 500,000 and 450,000 (Fig. 1B, lane 1) This finding is in accord with similar results reported previously by one of us (41) and others (34,40), and we have designated the apparently larger (slower mobility) subunit KLH-A, and the apparently smaller (faster mobility) subunit KLH-B.

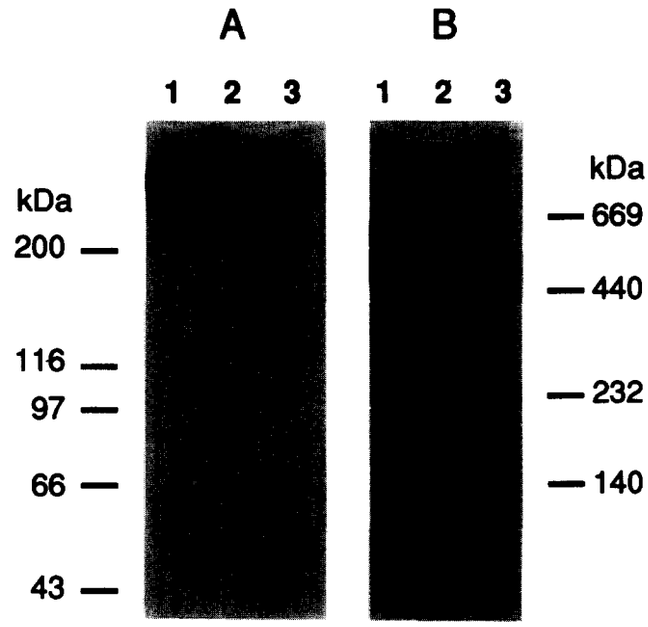

FIG. 1. Electrophoretic analyses of KLH in denaturing and nondenaturing polyacrylamide gels. (*A*) SDS-PAGE performed under reducing conditions; (*B*) Nondenaturing gradient gel electrophoresis under dissociating conditions. Lanes 1: purified KLH; Lanes 2, KLH-A (see also Fig. 2/Peak II); Lanes 3, KLH-B (see also Fig. 2/Peak I). Lanes were loaded with 4 μg of purified KLH or 2 μg of KLH-A or -B.

Identification of two electrophoretically distinct KLH subunits in an apparently homogeneous KLH preparation led us to determine whether it was possible to isolate each in quantity for further study. We found that high-performance anion exchange chromatography (HP-IEC) of the purified native protein resolved two major KLH isoforms (Fig. 2A, peaks I and II). The relative amounts of each isoform varied among KLH preparations, but generally ranged from 40–60% of each. Sedimentation-velocity measurements and electron microscopy (see below) established that both peaks contained fully assembled decamers and multi-decamers. Yields from the HP-IEC step were 70–80%, and minor peaks were collected and identified either as KLH monomers or fragments (not shown). Thus, >90% of the protein applied to this column was recovered, with the major fraction in peaks I and II. Interestingly, when the native protein was fully dissociated into subunits A and B, HP-IEC failed to resolve them (Fig. 2B).

SDS-PAGE of HP-IEC peaks I and II (Fig. 1A, lanes 2 and 3) yielded single major protein bands identical in mobility to that of the purified protein (Fig. 1A, lane 1). However, nondenaturing gel electrophoresis of Gly/EDTA-dissociated KLH from each of the two peaks (Fig. 1B, lanes 2 and 3)

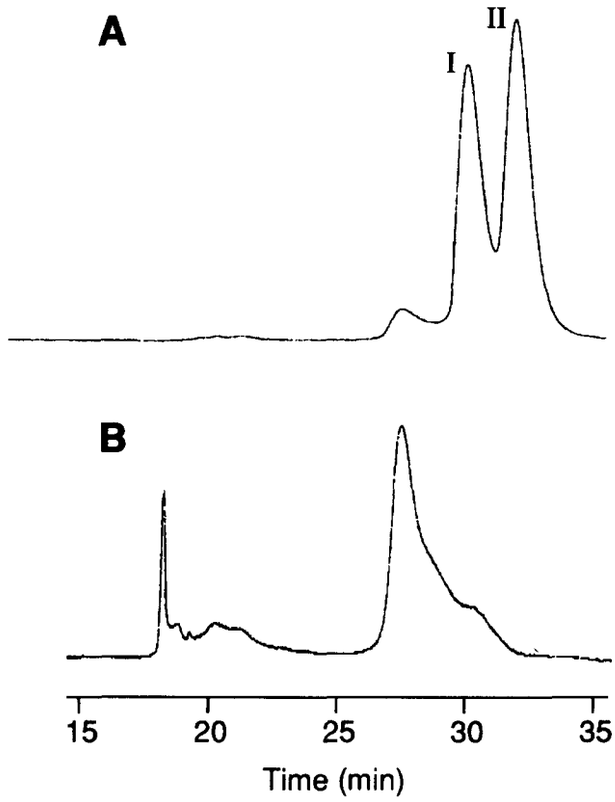

FIG. 2. High-performance anion-exchange chromatography (HP-IEC) (as described in Materials and Methods) resolves KLH-A and KLH-B. (*A*) Native purified KLH; (*B*) Dissociated KLH. The column effluent was monitored at 280 nm (0.2 AUFS).

disclosed that peak I was comprised entirely of KLH-B subunits, whereas peak II contained only KLH-A subunits.

The unanticipated conclusion from these results was that the purified KLH preparation actually consisted of two different multimeric proteins: one containing only subunit A (KLH-A) and the other containing only subunit B (KLH-B). Having resolved these two isoforms in quantity, it became possible to compare their structural and functional characteristics.

N-Terminal Sequences and Amino Acid Composition

N-terminal sequence analysis (Fig. 3) disclosed major differences between KLH-A and KLH-B, although both proteins exhibited significant homology to other molluscan hemocyanins. Amino acid analysis also provided evidence of significant differences between KLH-A and KLH-B, which agreed in mol-percent composition for only 3 of 14 amino acids (Table 1). A comparison of acidic (Asx, Glx) and basic (Lys, His, Arg) residues in the two proteins suggests that KLH-A has a lower isoelectric point than KLH-B. This may explain why KLH-A elutes after KLH-B on HP-IEC at pH 6.5 (Fig. 2),

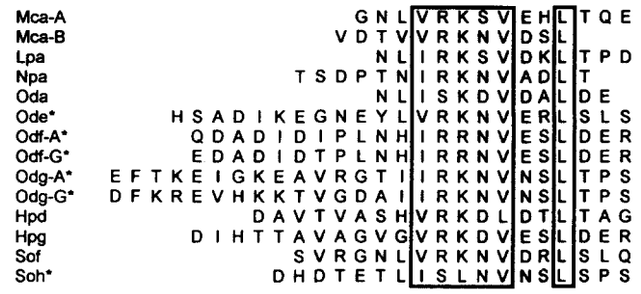

FIG. 3. N-terminal sequences of KLH-A and KLH-B are related to each other and to other mollusc hemocyanins. The nomenclature for oxygen binding domain sequences consists of a code representing genus and species, domain (a–h) and if more than one subunit or sequence is known—a designation for that type. Hence Mca-A is *Megathura crenulata* domain a, from subunit A. Lpa is *Loligo pealei* a; Npa, *Nautilus pompilius* a; Od, *Octopus dofleini*, includes sequences from A-type and G-type isoforms; Hp; *Helix pomatia*; So, *Sepia officinalis*. * denotes sequence determined from cDNA. Sequences come from the following sources. Hpd: Drexel *et al.* (16), Hpg: Xin *et al.* (50), Sof: Top *et al.* (43), Soh: Declercq *et al.*(9), Odf and Ode: Lang (30), Odg: Lang and van Holde (31), Oda, Lpa, Npa, Odc and Odd: Miller, Lang, and Varga-Weisz, unpublished.

but does not account for the faster mobility of KLH-B on native-gel electrophoresis (Fig. 1).

Sedimentation Coefficients and Molecular Weights

In an effort to further clarify the question of molecular weight, subunits obtained from dissociated KLH-A and KLH-B were examined by analytical ultracentrifugation. KLH-A exhibited

TABLE 1. Amino acid analysis of KLH-A and KLH-B

Amino acid	Mol-percent (Mean ± Std. Dev.) KLH-A	KLH-B	KLH-A versus KLH-B Mann-Whitney (p value)
Asx*	17.3 ± 0.42	14.4 ± 0.72	0.05
Thr*	5.82 ± 0.25	4.54 ± 0.12	0.05
Ser*	6.03 ± 0.21	6.89 ± 0.14	0.05
Glx*	13.6 ± 0.09	12.2 ± 0.13	0.05
Gly*	6.33 ± 0.18	7.00 ± 0.18	0.05
Ala*	8.15 ± 0.36	8.90 ± 0.35	0.05
Val*	4.45 ± 0.32	5.24 ± 0.18	0.05
Ile*	3.65 ± 0.08	3.95 ± 0.11	0.05
Leu	11.2 ± 0.18	10.9 ± 0.21	0.28
Tyr*	2.58 ± 0.13	4.57 ± 0.22	0.05
Phe	7.00 ± 0.40	6.84 ± 0.12	0.83
Lys	4.61 ± 0.14	4.59 ± 0.12	0.83
His*	7.40 ± 0.32	5.99 ± 0.08	0.05
Arg*	1.82 ± 0.42	3.91 ± 0.43	0.05

Samples (300 μg of KLH-A or KLH-B) were hydrolyzed in 6 N HCl plus 2% phenol for 20 h at 100°C. Mol-percent values were estimated from triplicate determinations of 5 μg of hydrolyzed protein. Sample means were compared via a nonparametric (Mann-Whitney two sample test, Glantz, 18) statistical method. * Denotes significant difference between KLH-A and KLH-B ($p \leq .0.05$).

significant size heterogeneity in sedimentation velocity runs below pH 10.0, suggesting the presence of an equilibrating mixture of monomers and dimers. However, by raising the pH to 10.7, a homogeneous boundary could be obtained. The molecular weight of this component was determined to be 4.49×10^5 daltons. KLH-B gave a fully dissociated subunit at pH 10 with a molecular weight of 3.92×10^5 daltons. The fitted data for the two subunits is contained in Fig.4.

Comparative Peptide Mapping

Lysylendoproteinase-C digests of KLH-A and KLH-B were evaluated by reversed-phase HPLC and SDS-PAGE. Reversed-phase HPLC (Fig. 5) disclosed three major peptides

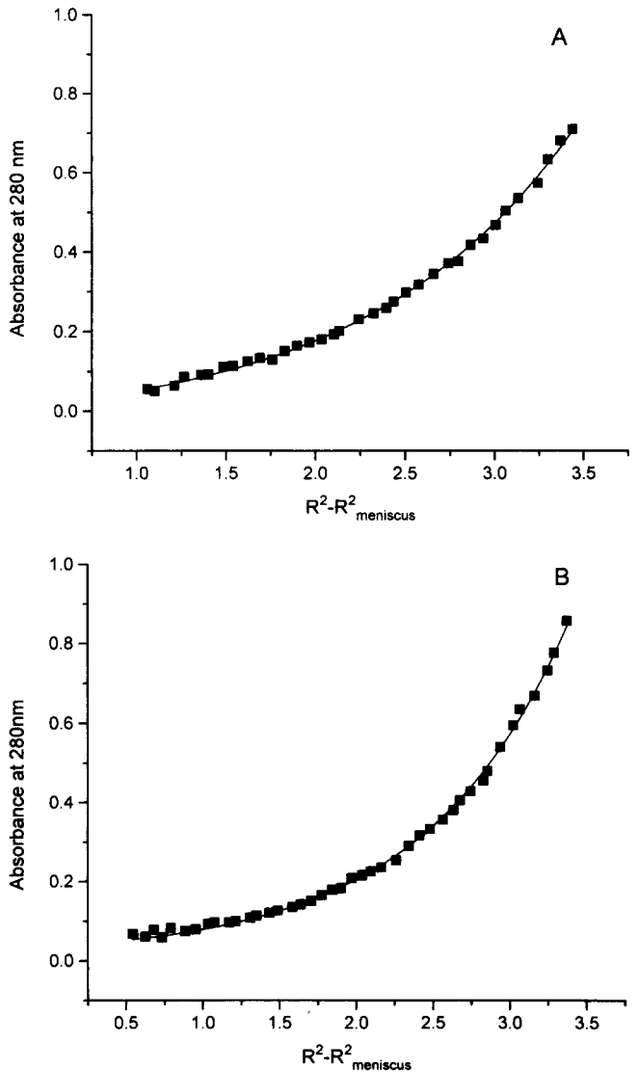

FIG. 4. Determination of molecular weights by analytical ultracentrifugation for KLH-A (A) and KLH-B (B). Experimental points from sedimentation equilibrium runs accurately fit the theoretical curve for a single component. Molecular weights are 4.49×10^5 for KLH-A and 3.92×10^5 for KLH-B.

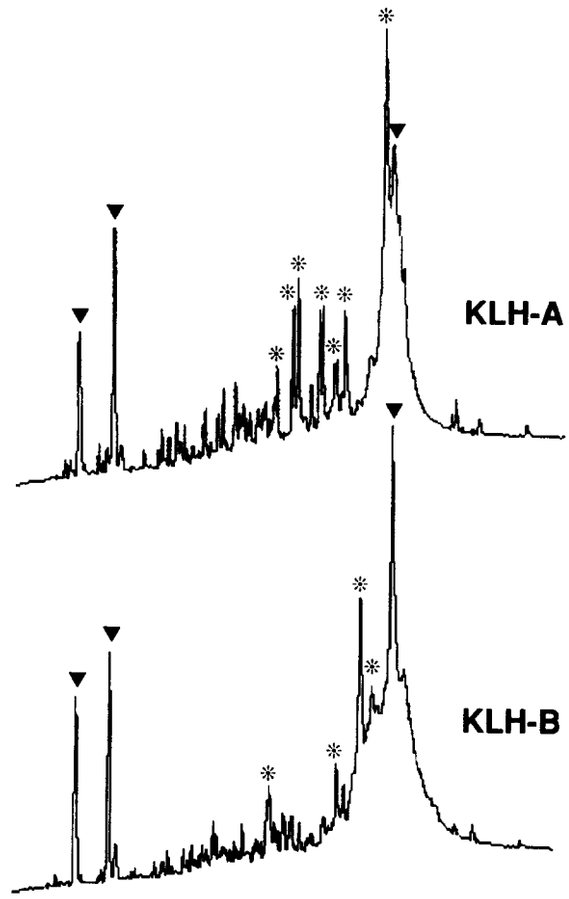

FIG. 5. Peptide mapping of KLH-A and KLH-B by reversed-phase HPLC. Asterisks denote unique peptides; triangles denote common peptides.

from KLH-A and KLH-B that coeluted and at least eleven unique peptides. SDS-PAGE of this same digest (Fig. 6) indicated that KLH-B was more resistant to proteolysis than KLH-A, and also revealed major differences between the two isoforms. Collectively these results support the conclusion that KLH-A and KLH-B have related but substantially dissimilar structures.

Copper Content

Molluscan hemocyanins typically contain about 0.25% copper by weight (46,48). KLH-A and KLH-B were analyzed by inductively coupled plasma emission spectroscopy and found to contain 0.21 and 0.25% copper (corresponding to 2.96 μg/ml copper and 1.4 mg/ml protein for KLH-A, and 2.96 μg/ml copper and 1.2 mg/ml protein for KLH-B). If one assumes KLH-A and KLH-B each contain eight oxygen binding domains/subunit, these values and the molecular weights reported above correspond to 2.0 Cu/domain for KLH-A and 2.1 Cu/domain for KLH-B (See Discussion and Table 2).

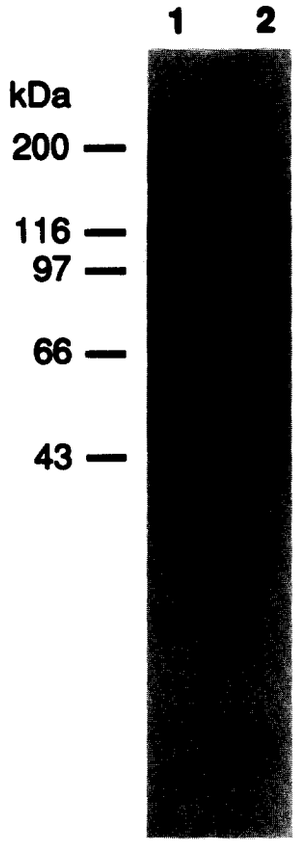

FIG. 6. Peptide mapping of KLH-A and KLH-B by SDS-PAGE. Proteolysis and electrophoresis conditions are described in Experimental Procedures. Lane 1, digest of KLH-B; lane 2, digest of KLH-A.

Oxygen Binding

Studies of oxygen binding equilibria provided additional evidence of dissimilarities between the two isoforms. As summarized in Fig. 7A, KLH-A exhibited almost three-fold lower oxygen affinity, as indicated by it's higher P_{50}, and somewhat less positive cooperativity, indicated by it's lower n_{50}, than KLH-B. The most likely explanation for such major functional differences is that the O_2 binding domains of KLH-A and KLH-B are quite different in primary structure.

Although the O_2 affinity of purified KLH (a 60:40 mixture of KLH-A and KLH-B), is intermediate between that of KLH-A and KLH-B, the cooperativity was less for the unfractionated material than for either isoform. However n_{max}, determined for the steepest portion of the Hill slope is clearly much greater than n_{50}. It is possible to show that such a complex curve results not from interaction between the two forms but from the simple mixing of two independent, non-equilibrating isoforms of different oxygen affinities. Theoretical curves derived from models in Wyman and Gill (49) are shown in Fig. 7B. They predict the experimental data we present. When the two isoforms are present in roughly equimolar amounts, the apparent cooperativity (measured as n_{50}) for the composite curve decreases. Figs. 7A and B show this reduced slope clearly. This highlights a potential difficulty of using n_{50} to characterize a mixture of proteins. The binding curve does not represent the real behavior of any particular protein but the mathematical combination of the behaviors of the components of the mixture. A similar phenomenon is responsible for apparent negative cooperativity in the *Octopus* hemocyanin subunit in which noncooperative oxygen binding units of different oxygen affinities are found (37).

TABLE 2. Predicted and observed copper content of KLH subunits

KLH type	Molecular weight[a] daltons	Predicted copper[b] μg/ml			Observed copper[c] μg/ml
A	449,000	3.31 (9)	2.94 (8)	—	2.96 ± 0.12
B	392,000	—	2.88 (8)	2.52 (7)	2.96 ± 0.09

[a]From sedimentation equilibrium.
[b]Calculated assuming 2 Cu/domain for the number of domains shown in parentheses.
[c]Mean and standard deviation from 3 measurements of each sample on a Jarrell-Ash Model 955 ICP Mass Spectrometer. The error in the measurement is <4%. Protein concentration was 1.4 and 1.2 mg/ml for KLH-A and KLH-B.

Structure and Dissociation/Reassociation Behavior by Electron Microscopy

Didecameric forms of KLH-A and KLH-B were indistinguishable under the electron microscope (Fig. 8, Panels A, C,

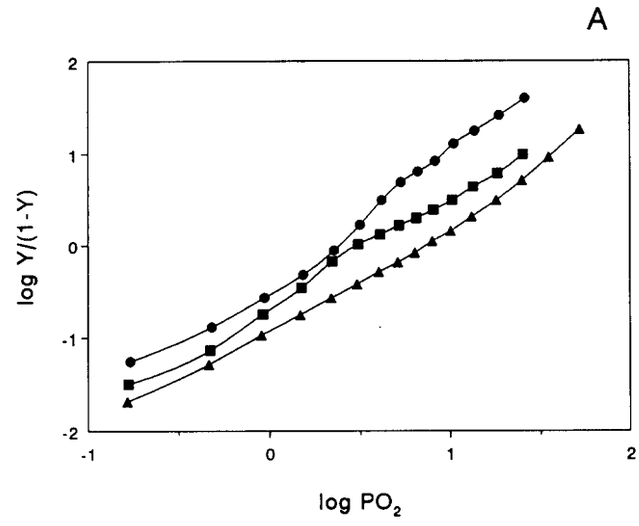

FIG. 7A. Hill Plot for oxygen binding to KLH. Oxygen binding of KLH-A (triangles), KLH-B (circles), and the mixture containing approximately 60% KLH-A and 40% KLH-B (squares) was measured in a PBS buffer at pH 7.3. Extrapolated values for the partial pressure of O_2 at half-saturation (P_{50}) were 7.32 for KLH-A, 2.46 for KLH-B, and 3.26 for the mixture. The Hill coefficients (n_{50}), extrapolated from the slopes of the curves at P_{50}, were1.40 for KLH-A, 1.94 for KLH-B, and 1.17 for the mixture.

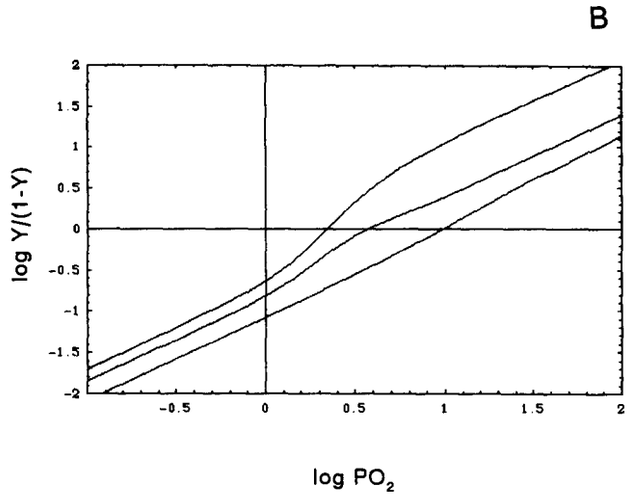

FIG. 7B. Simulated oxygen binding curves for two different hemocyanin molecules and of a noninterconverting ("frozen") mixture of the two (see, e.g., 49). Both hemocyanins are modelled as octameric MWC macromolecules, with binding polynomials $P_i = ((1 + k_{Ri}\,x)^8 + Li(1 + K_{Ti}\,x)^8)/(1 + L_i)$ for each subpopulation i = 1,2. Here x is the oxygen activity, k_R and k_T are the oxygen association constants for the R and T state octamer, and L is the equilibrium constant for the allosteric transition R → T. The binding polynomial for a mixture with an equal proportion of subpopulations 1 and 2 is $P_m = P_1^{1/2} P_2^{1/2}$. The fractional oxygen saturations (Y) and the Hill plots are calculated in the normal way. *Left curve*: Population 1 only; $k_R = 1.2$ torr^{-1}, $k_T = 0.2$ torr^{-1}, L = 2000. *Right curve*: Population 2 only; $k_R = 0.16$ torr^{-1}, $k_T = 0.08$ torr^{-1}, L = 30. *Middle curve*: Quantities calculated for an equal-proportion mixture of populations 1 and 2.

& D). However, the two isoforms appeared to differ in the distribution of multimers: KLH-A was present for the most part in decameric and didecameric forms, with a few multidecamers visible (Fig. 8C), whereas KLH-B, although mainly present as a didecamer, contained relatively higher amounts of large, extended multimers (Fig. 8D). This tendency also was evident in a dissociation/reassociation experiment (see below for experimental details) wherein we found that KLH-B exhibited a clear bias towards formation of the extended multimers (compare Figs. 8E and 8F).

Structure and Dissociation/Reassociation Behavior by Sedimentation-Velocity Ultracentrifugation and HP-IEC

Analytical ultracentrifugation of purified KLH (Fig. 9A and Table 3) indicated that about 90% was present in decameric or didecameric multimers, with the remainder in the form of extended multimers. Virtually all of this preparation was dissociable into monomers following dialysis against Gly/EDTA buffer (Figs. 8B and 9G). To study and compare their polymerization characteristics in solution, purified KLH, KLH-A, and KLH-B were fully dissociated to their monomeric forms by dialysis (at 20°C) against Gly/EDTA buffer and then

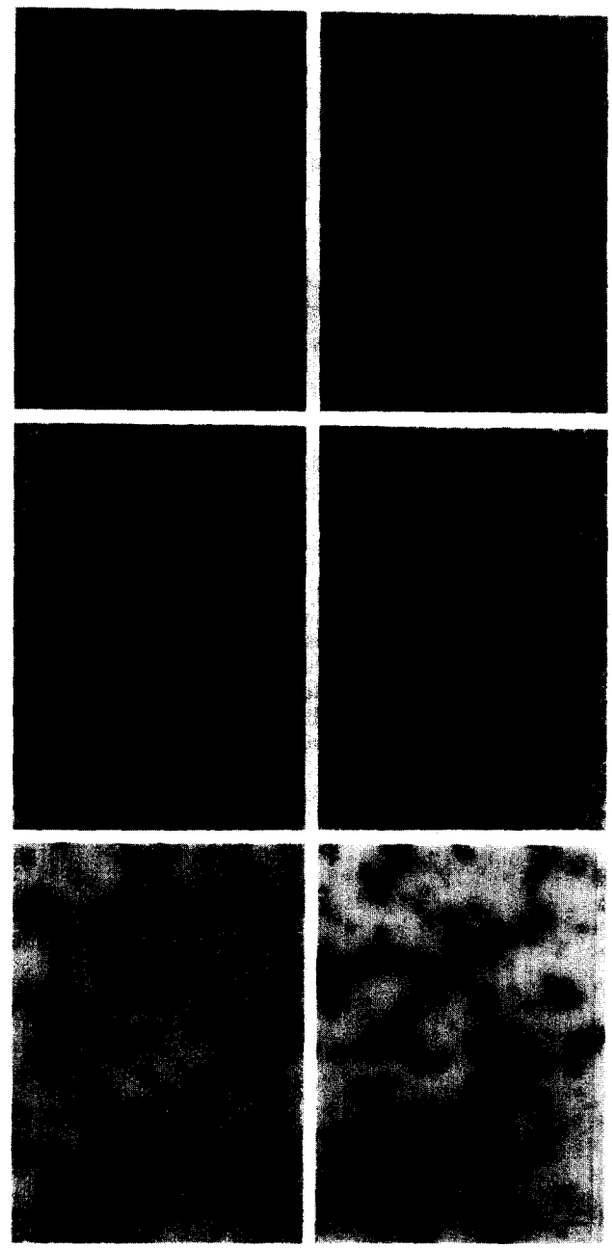

FIG. 8. Electron microscopy of KLH. (*A*) Purified KLH (containing both KLH-A and KLH-B). Arrows denote large polymeric structures (m.w. >40 million); solid triangles: didecamers (m.w. ~9 million); open triangles: decamers (m.w. ~4.5 million). Circular structures represent cross-sectional views that illustrate the "tubular polymer" nature of KLH multimers. (*B*) Dissociated KLH. (*C*) KLH-A. (*D*) KLH-B. (*E*) Reassociated KLH-A. (*F*) Reassociated KLH-B.

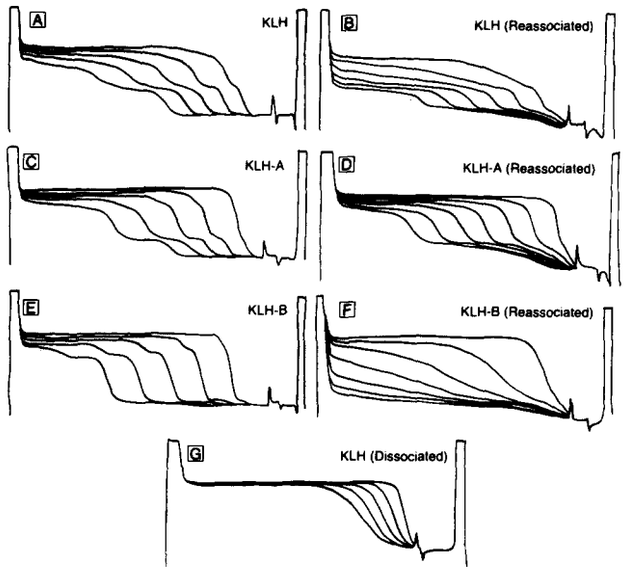

FIG. 9. Sedimentation velocity ultracentrifugation of purified KLH, KLH-A, and KLH-B in native, dissociated, and reassociated forms. Direction of sedimentation is from right to left. Scans were performed at 12 min intervals. Protein concentration is proportional to plateau heights, and homogeneity is greatest when the boundaries between plateaus are steep. Sedimentation coefficients estimated from panels A, C, and E are shown in Table 3. For example, in panel E, the fastest boundary corresponds to a sedimentation coefficient of 105S, and in panel G, the boundary corresponds to 11–13S.

allowed to reassociate during dialysis against 0.1 I Tris pH 7.65 containing (10 mM) $CaCl_2$ and (50 mM) MgC_2l. This procedure provided evidence of major differences in reassociation behavior (Compare Figs. 9A, 9C, and 9E with Figs. 9B, 9D, and 9F): Initially, undissociated KLH-A was about equally distributed between decameric and didecameric forms with a small amount (<1%) of multidecamers (Fig. 9C; Table 3). Dissociated (~13S) KLH-A subunits reassociated almost completely to their original composition of didecamers, and also contained dimers and decamers (Fig. 9D); this size distribution was confirmed by electron microscopy (Fig. 8E). Later reassociation experiments on KLH-A, using material fully dissociated (~11S) for sedimentation equilibrium showed identical reassociation behavior (not shown). In contrast, KLH-B, which originally contained about 80% didecamers (Fig. 8E and Table 3), reassociated to a very heterogeneous mixture of exceptionally large molecules (Fig. 9F and Table 3) that corresponded to extended multimers in the electron microscope (Fig. 8F). Thus, if one defines successful reassociation as restoration of the original sedimentation-velocity pattern, KLH-A reassociated better than KLH-B under the conditions of this experiment. Importantly, the tendency to form extended multimers appears to be a characteristic of reassociated KLH-B. This observation suggests that extended multimers commonly found in hemolymph may contain primarily KLH-B.

In an attempt to determine whether the reassociation products contained heteropolymers, material subjected to the dissociation/reassociation process described above was analyzed by HP-IEC as before. The reassociation buffer, 50 mM Tris pH 7.5 with 100 mM NaCl, 10 mM $CaCl_2$, and 5 mM $MgCl_2$ differed from the reassociation conditions previously described in the levels of divalent cations present. These new conditions were chosen to provide excess levels of divalent cations for reassociation, and to resemble more closely the divalent cation conditions in the buffer used to resolve KLH-A and KLH-B native molecules by HP-IEC. Fig. 10B shows the profile obtained after reassociation. The two major peaks (fractions 29 and 31) have the same elution times as native KLH-B and KLH-A (Fig. 10A). Nondenaturing gels (Fig. 11) revealed that fraction 29 contained KLH-B and fraction 31 contained KLH-A. Shoulders (fractions 27 and 28) contained only KLH-B in less aggregated forms. No form isolated by HP-IEC contained both types of KLH subunit. Table 4 shows the aggregation state of the KLH isolated from these peaks and shoulders.

DISCUSSION

We have provided direct evidence that the two distinct respiratory proteins from the giant keyhole limpet (KLH-A and KLH-B) differ in (i) primary structure, as evidenced by N-terminal sequencing, amino acid analysis, and comparative peptide mapping; (ii) polymerization-reassociation characteristics, as indicated by electron microscopy and sedimentation velocity ultracentrifugation; and (iii) O_2 binding characteristics. Amino acid composition, N-terminal sequences, and peptide maps clearly indicate that the two subunits are different hemocyanins. Since we have no information about the carbohydrate content of KLH-A and -B, we cannot rule out a contribution by oligosaccharides to some of the observed differences in the electrophoretic and chromatographic mobilities of intact KLH-Aand -B or their peptide fragments. Nevertheless, we think the structural and functional evidence is strong enough to indicate that KLH-A and KLH-B are different gene products.

TABLE 3. Size distribution of KLH by sedimentation-velocity ultracentrifugation[a]

Sample	Monomer	Decamer	Didecamer	>Didecamer
KLH[b]	—	35% (63S)	55% (105S)	10% (≥125S)
KLH-A	—	50% (67S)	50% (100S)	<1% (≥125S)
KLH-B	—	5% (61S)	80% (105S)	15% (≥129S)

[a]Samples were analyzed in a Beckman Model E ultracentrifuge equipped with a photoelectric scanner. Results were analyzed according to van Holde & Weischet (47). These values were determined from the scans shown in Fig. 9A, C, and E.

[b]Purified KLH containing approx. 60% KLH-A and 40% KLH-B.

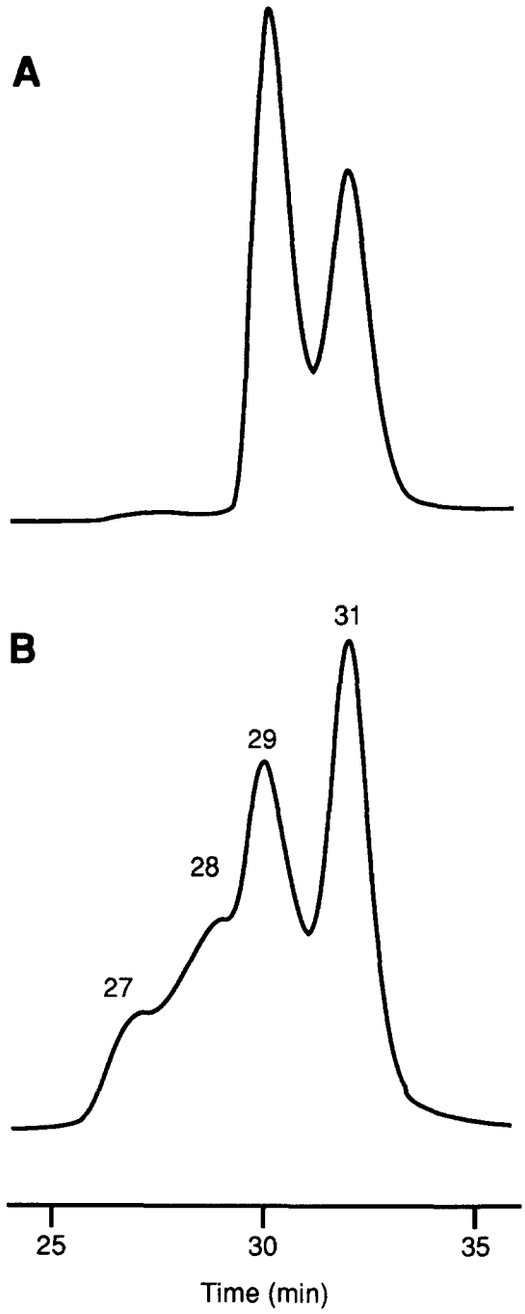

FIG. 10. HP-IEC of native and reassociated KLH. (*A*) Native purified KLH, 100 mg. This lot of KLH contained 60% KLH-B and 40% KLH-A. Column effluent was monitored at 280 nm (0.2 AUFS). (*B*) Reassociated KLH from the same lot as shown above, 1.0 mg. Column effluent was monitored at 280 nm (1.0 AUFS). Dissociation was done using Gly/EDTA buffer as described in Materials and Methods. Reassociation was done as described in Results. Four fractions, indicated by the numbers 27, 28, 29, and 31, were collected representing the peaks and shoulders. They were subsequently analyzed by nondenaturing electrophoresis (Fig. 11) and sedimentation velocity ultracentrifugation (Table 4).

TABLE 4. Aggregation state of peaks isolated by HP-IEC from reassociated native KLH

		% of each fraction as			
Fraction #	**Subunit**	**Dimer**	**Decamer**	**Didecamer**	**>Didecamer**
27	B	30	30	40	—
28	B	10	50	40	—
29	B	—	30	70	—
31	A	10	—	70	20

Both nondenaturing gels and sedimentation equilibrium suggest about 50 kDa difference in subunit size. While this difference makes it tempting to speculate that KLH-A contains one more O_2 binding domain than KLH-B, we do not believe this to be the case. At the present time there are no reported 7-domain subunits for any molluscan hemocyanins except for the cephalopods *Octopus* (29) and probably also *Nautilus* (36). The predicted copper contents for differing numbers of domains do not accurately reflect the observed copper levels for KLH-A and KLH-B. These copper levels best fit an eight-domain structure for both subunits (Table 2). Electron micrographs of KLH-A and KLH-B (Fig. 8) look identical to each other with respect to collar structure and identical to all other known 8-domain hemocyanins. In cephalopods, 7-domain hemocyanin subunits are easily distinguished from 8-domain subunits on the basis of the difference in density of collar structures in decameric hemocyanins (36).

If both subunits do have eight domains, these domains must be of different sizes, with an average molecular weight/domain of ~56,000 for KLH-A and ~49,000 for KLH-B. The sizes now accepted as accurate measurements for chiton and gastropod hemocyanin subunits range from ~400,000 to 480,000 daltons (45). For an 8 domain subunit, each domain would range from 50,000 to 60,000 daltons. It is certainly possible that KLH-A and KLH-B, evolving as separate genes in this primitive mollusc, could show such differences in molecular weight.

The process of determining unequivocally by chemical and immunological methods that a hemocyanin contains a specific number of domains is arduous and seldom undertaken. Limited proteolysis is necessary to separate domains for the production of antibodies. In our experience with *Octopus* (29), the N-terminal domain was so susceptible to proteolytic degradation that it was almost impossible to detect. One could have easily assumed for *Octopus* that the subunit contained one fewer domain than was found upon more careful examination. Electron microscopy under dissociating conditions has also been used to directly observe the number of domains in hemocyanin of *Octopus* and other molluscs. The highly alkaline conditions (pH $\geq$ 10) necessary to obtain fully unfolded KLH subunits in which individual domains are clearly visible makes negative staining for electron microscopy difficult. Therefore, seeing a chain that appears to contain seven globular domains does not prove that eight are not present unless many fully unfolded chains are observed and none contain

eight. Gebauer *et al.* (16) describe immunological and electron microscopic data suggesting KLH-B has seven domains, but in the light of the arguments just made we believe it premature to accept this model.

On the basis of available evidence we are convinced that KLH subunits contain eight-domains. Whether the increased molecular weight for KLH-A is distributed equally among the domains in the subunit, or is present only in a few has not been determined for KLH or any other gastropod hemocyanin. It is interesting to note in this regard that of the domains now sequenced for *Octopus* hemocyanin, all are close to 50,000 daltons (36) whereas the three domains sequenced for the β-hemocyanin of the gastropod *Helix pomatia* differ by the addition of nearly 200 amino acids to the C-terminal domain Hph (13). This corresponds to an increase in molecular weight of about 20,000 daltons.

Perhaps the most curious finding concerns reassociation of purified KLH (Fig. 9B). Our initial observation was that if the scans for reassociated KLH-A (Fig. 9D) and KLH-B (Fig. 9F) were superimposed, the composite closely resembled Fig. 9B. This suggested, somewhat indirectly, that subunits A and B reassociate independently even when mixed in solution and do not form heteropolymers composed of both subunits. Subsequent HP-IEC purification of reassociated material confirmed this hypothesis (Fig. 10). The peaks were collected and both native gels (Fig. 11) and sedimentation velocity profiles (Table 4) were made for the peaks and shoulders and the results clearly show that the material reassociates into homogeneous multimers, one peak containing only A, the other peak and shoulders only B. This is unequivocal evidence that subunits A and B reassociate independently even when mixed in solution. It is, to our knowledge, the first experimental evidence for this process.

When the two KLH isoforms are dissociated, reassociation does not yield a sedimentation profile identical to native material; KLH-A reassociates in mixed solution into a didecamer very like the native material (Fig. 9C). The KLH-B subunit does not reappear as exactly the same group of larger multimers (Fig. 9E). Studies are underway to examine the control of association to higher aggregation states. But it does reassociate with other B subunits and not into an array of mixed heteropolymers. What does this say about the production of these two isoforms by the cells which synthesize hemocyanins? In keyhole limpets there are two possibilities: either they are produced in the same cells, or they are produced in two different cell types. Seeing incomplete or poor reassociation in itself does not differentiate these two possibilities. If we had seen substantial formation of heteropolymers upon reassociation, we would have been forced to conclude that *in vivo* the two forms need to be produced separately, in either spatial (different cell types) or temporal (different times of synthesis) isolation from one another, in order to prevent the formation of heteropolymers, which are never seen in native material. Seeing instead very complete reassociation of two isoforms from a mixture of the two subunits we conclude that

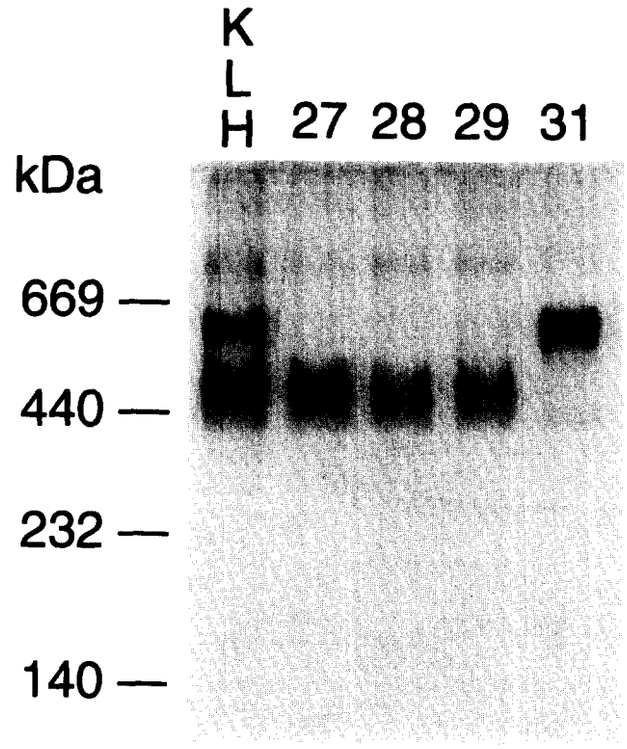

FIG. 11. Nondenaturing electrophoretic analysis of fractionated reassociation products. Lanes were loaded with 5 μg of unfractionated KLH protein, or 2.5 μg of protein from fractions 27, 28, 29, or 31 as indicated.

it is certainly possible that the same cell types could produce both types of hemocyanin, and that they are simply too different from one another to form stable hybrids. The nature of the ability of KLH-A and KLH-B to self-associate from a mixture will be the subject of future investigation.

Recent studies on the structure and architecture of KLH by Markl *et al.* (34) also demonstrated two electrophoretically and immunologically distinct forms of KLH. They succeeded in purifying their corresponding subunits by preparative alkaline PAGE and gel permeation chromatography. "Subunits 1 and 2" correspond to our KLH-A and KLH-B, respectively. They also observed a greater tendency on the part of Subunit 2 (KLH-B) to form extended multimeric structures. However, and in contrast to the results presented here, these authors initially claim to have observed three classes of KLH multimers: clustered didecamers containing subunit 1 (KLH-A); extended multi-decamers containing subunit 2 (KLH-B), and solitary didecamers containing both subunits in roughly equal proportions. They now find there are no heteropolymers (16). Thus both studies are in agreement, with the explanation for their early findings being simply that gel permeation chromatography isolated one peak containing the didecameric molecules from both subpopulations isolated by HP-IEC.

Ours is not the first disclosure of heterogeneity among hemocyanins. Herscowitz *et al.* (22) used anion-exchange chro-

matography to resolve two KLH isoforms that differed both in antigenicity and electrophoretic mobility. Moreover, Senozan *et al.* (41) detected two KLH isoforms on native gel electropherograms. However, in these and other previous publications, it was assumed that the observed heterogeneity reflected posttranslational modifications, and no evidence indicating that these isoforms differed in primary structure or functional characteristics was presented. Regarding other molluscan hemocyanins, at least two immunologically and functionally distinct isoforms have been reported for *Helix pomatia* (see 45), and cDNA sequencing has disclosed minor sequence differences in *Octopus dofleini* hemocyanins (Fig. 3 and Ref 31). Considering these data plus the results of the present study, it seems likely that hemocyanins from a given species may be more structurally heterogeneous than previously assumed, and that the presence of two or more isoforms with different functional characteristics may be a common feature of molluscan hemocyanins.

One specific implication from our results is that many if not all prior studies of physicochemical, functional, and immunologic properties of KLH must now be reinterpreted as representing an average result for two distinct proteins. Of broader significance is the question of whether molecular heterogeneity is a common feature of most molluscan hemocyanins. If so, then it will be interesting to know if such heterogeneity is associated with any selective advantages for the organism. It certainly suggests that hitherto unsuspected heterogeneity among the whole molecules may be responsible in part for the common observation of very slight apparent cooperativity of oxygen binding in molluscan hemocyanins. Significant cooperativity might have been observed had isolated isoforms been evaluated.

Finally, in view of the potential applications of KLH to vaccine development and cancer therapy, it may be important to determine whether the two isoforms have different immunostimulatory properties. Clearly there is much more to be learned, and we anticipate that the present study will serve as a basis for further elucidation of KLH structure and function.

We thank K. E. van Holde, Charles Robert, and J. Bonaventura for helpful comments and discussions regarding this work. Also, we are grateful to J. D. Robertson and the Departments of Cell Biology and Neurobiology at Duke University Medical Center for the use of electron microscope facilities, and to R. McParland at Oregon State University for protein sequencing and amino acid analyses. This work was supported, in part, by NSF Grant No. MC93-05250 and NIEHS Center Grant No. ESO-1908.

References

1. Amkraut, A.A.; Malley, A.; Begley, D. Immunogenicity of hemocyanins and their subunits. J. Immunol. 103:1301–1310;1969.
2. Bagasra, O.; Forman, L.J.; Howeedy, A.; Whittle, P. A potential vaccine for cocaine abuse prophylaxis. Immunopharmacology 23:173–179;1992.
3. Bartel, A.H.; Campbell, D.H. Some immunochemical differences between associated and dissociated hemocyanin. Arch. Biochem. Biophys. 82:232–234;1959.
4. Bird, P.; Calvert, J.E.; Amlot, P.L. Distinctive development of IgG_4 subclass antibodies in the primary and secondary responses to keyhole limpet haemocyanin in man. Immunol. 69:355–360;1990.
5. Campbell, D.H.; Garvey, J.S.; Cremer, N.E.; Sussdorf, D.H. Meth. Immunol. New York: WA Benjamin, Inc. 69–71;1963.
6. Campbell, W.P.; Wrigley, C.W.; Margolis, J. Electrophoresis of small proteins in highly concentrated and crosslinked polyacrylamide gradient gels. Anal. Biochem. 129:31–36;1983.
7. Curtis, J.E.; Hersh, E.M. The human secondary immune response to keyhole limpet haemocyanin. Clin. Exp. Immunol. 10:171–177;1972.
8. Curtis, J.E.; Hersh, E.M.; Harris, J.E.; McBride, C.; Freireich, E.J. The human primary immune response to keyhole limpet haemocyanin: Interrelationships of delayed hypersensitivity, antibody response and in vitro blast transformation. Clin. Exp. Immunol. 6:473–491;1970.
9. Declercq, L.; Witters, R.; Preaux, G. Partial sequence determination of *Sepia officinalis* hemocyanin via cDNA. In: Preaux, G.; Lontie, R., eds. Invertebrate dioxygen carriers. Leuven: Leuven University Press; 1990:131–134.
10. Dixon, F.J.; Jacot-Guillarmod, H.; McConahey, P.J. The antibody responses of rabbits and rats to hemocyanin. J. Immunol. 97:350–355;1966.
11. Drexel, R.; Siegmund, S.; Schneider, H.J.; Linzen, B.; Gielens, C.; Preaux, G.; Kéllerman, J.; Lottspeich, F. Complete amino acid sequence of a functional unit from molluscan hemocyanin (*Helix pomatia*). Biol. Chem. Hoppe-Seyler 368:617–635;1987.
12. Ellerton, H.D.; Ellerton, N.F.; Robinson, H.A. Hemocyanin-A current perspective. Prog. Biophys. Molec. Biol. 41:143–248;1983.
13. Finotto, M.; Gielens, C.; Witters, R.; Van Beeumen, J.; Preaux, G. Amino acid sequence of the C-terminal part of functional unit h from the β_c-haemocyanin of *Helix pomatia*. In: Preaux, G.; Lontie, R., eds. Invertebrate dioxygen carriers. Leuren: Leuren University Press; 1990:107–111.
14. Flamm, J.; Bucher, A.; Höltl, W.; Albrecht, W. Recurrent superficial transitional cell carcinoma of the bladder: Adjuvant topical chemotherapy versus immunotherapy. A prospective randomized trial. J. Urol. 144:260–263;1990.
15. Fredericq, M.L. Sur l'hémocyanine, substance nonvelle du sang de Poulpe (*Octopus vulgaris*) C.r hebol séanc. Acad. Sci. Paris 87:996–998;1878.
16. Gebauer, W.; Harris, J.R.; Heid, H.; Süling, M.; Hillenbrand, R.; Söhngen, S.; Wegener-Strake, A.; Markl, J. Quaternary structure, subunits and domain patterns of two discrete forms of keyhole limpet hemocyanin: KLH 1 and KLH 2. Zoology 98:51–68;1994.
17. Ghiretti-Magaldi, A.; Ghiretti, F. The pre-history of hemocyanin. The discovery of copper in the blood of molluscs. Experientia 48:971–972;1992.
18. Glantz, S.A. Primer of biostatistics, 3rd ed. New York: McGraw-Hill, Inc.; 1992.
19. Green, A.A.; Borella, L. *In vitro* response of human leukocytes to associated and dissociated hemocyanin. J. Immunol. 107: 293–297;1971.
20. Harris, J.R.; Gebauer, W.; Markl, J. Immunoelectron microscopy of hemocyanin from the keyhole limpet (*Megathura crenulata*): a parallel subunit model. J. Struct. Biol. 111:96–104;1993.
21. Haurowitz, F.; Hardin, R.L. Hemocyanin. In: Neurath, H.; Bailey, K., eds. The proteins. New York: Academic Press; 1954: 336–344.
22. Herscowitz, H.B.; Harold, W.W.; Stavitsky, A.B. Immunochemical and immunogenic properties of a purified keyhole limpet haemocyanin. Immunology 22:51–61;1972.
23. Herskovits, T.T. Recent aspects of the subunit organization and

dissociation of hemocyanins. Comp. Biochem. Physiol. 91B: 597–611;1988.
24. Jurincic, C.D.; Engelmann, U.; Gasch, J.; Klippel, K.F. Immunotherapy in bladder cancer with keyhole-limpet hemocyanin: a randomized study. J. Urol. 139:723–726;1988.
25. Kahn, J.O.; Stites, D.P.; Scillian, J.; Murcar, N.; Stryker, R.; Volberding, P.A.; Naylor, P.H.; Goldstein, A.L.; Sarin, P.S.; Simmon, V.F.; *et al.* A phase I study of HGP-30, a 30 amino acid subunit of the human immunodeficiency virus (HIV) p17 synthetic peptide analogue sub-unit vaccine in seronegative subjects. AIDS. Res. Hum. Retroviruses 8:1321–1325;1992.
26. Kälble, T.; Möhring, K.; Ikinger, U.; Riedasch, G.; Staehler, G. Intravesikale rezidivprophylaze beim oberflachlichen harnblasenkarzinom mit BCG und KLH. Urologe 30:118–121;1991.
27. Laemmli, U.K. Cleavage of structural proteins during the assembly of the head of bacteriophage T4. Nature 227:680–685;1970.
28. Lamm, D.L.; DeHaven, J.I.; Riggs, D.R.; Ebert, R.F. Immunotherapy of murine bladder cancer with keyhole limpet hemocyanin (KLH). J. Urol. 149:648–652;1993.
29. Lamy, J.; Leclerc, M.; Sizaret, P.-Y.; Lamy, J.; Miller, K.I.; McParland, R.; Van Holde, K.E. *Octopus dofleini* hemocyanin: Structure of the seven-domain polypeptide chain. Biochemistry 26:3509–3518;1987.
30. Lang, W.H. cDNA cloning of the *Octopus dofleini* hemocyanin: sequence of the carboxyl terminal domain. Biochemistry 27: 7276–7282;1988.
31. Lang, W.H.; van Holde, K.E. Cloning and sequencing of *Octopus dofleini* hemocyanin cDNA: derived sequences of functional units Ode and Odf. Proc. Natl. Acad. Sci. USA 88:244–248;1991.
32. Long, C. The biochemists handbook. Princeton, NJ: Van Nostrand; 1961.
33. Lowry, O.H.; Rosebrough, N.J.; Farr, A.L.; Randall, R.J. Protein measurement with the folin phenol reagent. J. Biol. Chem. 193:265–275;1951.
34. Markl, J.; Savel-Niemann, A.; Wegener-Strake, A.; Suling, M.; Schneider, A.; Gebauer, W.; Harris, J.R. The role of two distinct subunit types in the architecture of keyhole limpet hemocyanin (KLH). Naturwiss. 78:512–514;1991.
35. Mattson, J.R.; Roberts, M.; Patterson, R. Respiratory immune response to aerosolized keyhole limpet hemocyanin in primate lungs. Infect. Immun. 9:708–713;1974.
36. Miller, K.I. Cephalopod haemocyanins. A review of structure and function. Mar. Behav. Physiol. 25:101–120;1994.
37. Miller, K.I.; Van Holde, K.E. Oxygen-linked dissociation and oxygen binding by subunits of *Octopus dofleini* hemocyanin. In: Linzen, B., ed. Invertebrate oxygen carriers. Berlin: Springer-Verlag; 1986:417–420.
38. Riggs, A.F.; Wolbach, R.A. Sulfhydryl groups and the structure of hemoglobin. J. Gen. Physiol. 39:585–605;1956.
39. Salvaggio, J.; Castro-Murillo, E.; Kundur, V. Immunologic response of atopic and normal individuals to keyhole limpet hemocyanin. J. Allergy 44:344–354;1969.
40. Savel-Niemann, A.; Wegener-Strake, A.; Markl, J. Keyhole limpet hemocyanin: On the structure of a widely used immunologic tool. In: Preaux, G.; Lontie, R., eds. Invertebrate dioxygen carriers. Leuven: Leuven University Press; 1990:351–356.
41. Senozan, N.M.; Landrum, J.; Bonaventura, J.; Bonaventura, C. Hemocyanin of the giant keyhole limpet, *Megathura crenulata.* In: Lamy, J.; Lamy, J., eds. Invertebrate oxygen-binding proteins. New York: Marcel Dekker; 1981:703–717.
42. Swerdlow, R.D.; Ratliff, T.L.; La Regina, M.; Ritchey, J.K.; Ebert, R.F. Immunotherapy with keyhole limpet hemocyanin: efficacy and safety in the MB-49 intravesical murine bladder tumor model. J. Urol. 151:1718–1722;1994.
43. Top, A.; Gielens, C.; Witters, R.; van Beumen, J.; Preaux, G. Partial amino acid sequence and location of the carbohydrate chain in functional unit of *Sepia officinalis.* In: Preaux, G.; Lontie, R., eds. Invertebrate dioxygen carriers. Leuven: Leuven University Press; 1990:119–124.
44. Van Holde, K.E.; Miller, K.I. Hemocyanins Quart. Rev. Biophys. 15:1–129;1982.
45. Van Holde, K.E.; Miller, K.I.; Lang, W.H. Molluscan hemocyanins: Structure and function. Adv. Comp. Environ. Physiol. 13:257–300;1992.
46. Van Holde, K.E.; Van Bruggen, E.F.J. The Hemocyanins. In: Timasheff, S.N.; Fasman, G.D., eds. Subunits in biological systems. New York: Marcel Dekker; 1971:1–53.
47. Van Holde, K.E.; Weischet, W.O. Boundary analysis of sedimentation-velocity experiments with monodisperse and paucidisperse solutes. Biopolym. 17:1387–1403;1978.
48. Vandenbark, A.A.; Yoshihara, P.; Carveth, L.; Burger, D.R. All KLH preparations are not created equal. Cell. Immunol. 60:240–243;1981.
49. Wyman, J.; Gill, S. Binding and linkage. Mill Valley, CA: University Science Books; 1990:82.
50. Xin, X.Q.; Gielens, C.; Witters, R.; Preaux, G. Amino acid sequence of the functional unit g from β_c-hemocyanin of *Helix pomatia.* In: Preaux, G.; Lontie, R., eds. Invertebrate dioxygen carriers. Leuven: Leuven University Press; 1990:113–118.